REPORT 994

ANALYSIS OF SPANWISE TEMPERATURE DISTRIBUTION IN THREE TYPES OF AIR-COOLED TURBINE BLADE

By JOHN N. B. LIVINGOOD and W. BYRON BROWN

SUMMARY

Methods for computing spanwise blade-temperature distributions are derived for air-cooled hollow blades, air-cooled hollow blades with inserts, and air-cooled blades containing internal cooling fins. Individual and combined effects on spanwise blade-temperature distributions of cooling-air-temperature change due to heat transfer and rotation, radiation, and radial heat conduction are determined. In general, the effects of radiation and radial heat conduction were found to be small and the omission of these variations permitted the construction of nondimensional charts for use in determining spanwise temperature distributions through air-cooled turbine blades.

An approximate method for determining the allowable stress-limited blade-temperature distribution is included, with brief accounts of a method for determining the maximum allowable effective gas temperatures and the cooling-air requirements. Numerical examples that illustrate the use of the various temperature-distribution equations and of the nondimensional charts are also included.

INTRODUCTION

One of the most important limitations imposed on the design and the performance of aircraft gas-turbine power plants is the strength of the turbine materials; this strength decreases as the temperature increases. Turbine cooling offers the possibility of removing this limitation, even with the use of nonstrategic materials. Because of its relative simplicity, the passing of air radially through the turbine has been the subject of considerable investigation.

Theoretical and experimental studies made independently in Germany, England, and the United States showed that the circulation of cool air through hollow blades (fig. 1(a)) would allow the blades to operate several hundred degrees below the effective gas temperature. Experiments with inserts showed further that the required amount of cooling air could be considerably reduced if an insert (fig. 1(b)) was used to block off the central part of the hollow-blade air passage.

Knowledge of the temperature distribution through a turbine of known design and operating conditions is important. The predominant temperature gradients for air-cooled blades are radial in direction. An analytical investigation of this distribution was completed in 1949 at the NACA Lewis laboratory and is reported herein.

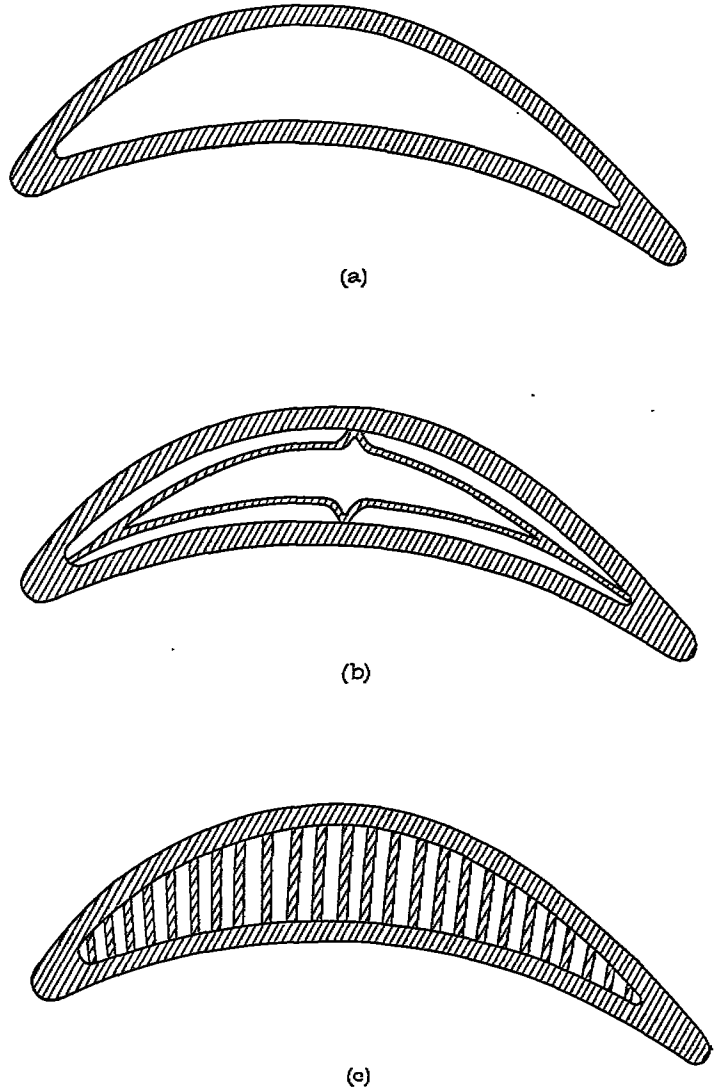

(a) Hollow blade.
(b) Insert blade.
(c) Finned blade.

FIGURE 1.—Cooling-passage configurations for air-cooled turbine blades.

A one-dimensional spanwise equation for blade-temperature distribution is derived for an air-cooled blade with an insert; allowance is made in this equation for changes in cooling-air temperature due to heat transfer and rotation,

radiation, and radial heat conduction through the blade metal. Modifications are made to adapt the equation to the calculation of temperature distribution in hollow blades and in hollow blades with internal cooling fins.

The relative importance of the terms due to rotation, radiation, and radial heat conduction is evaluated by omitting the last three factors of the spanwise equation, one at a time. A number of simplified solutions, which are adequate for many purposes, are thereby obtained. These simplified solutions permit the use of nondimensional charts, which give the temperature distribution with a minimum of calculation in all cases where radiation and radial conduction can be neglected.

An approximate method for determining the allowable stress-limited blade-temperature distribution is also presented and is used with the calculated blade-temperature distribution to find the maximum allowable effective gas temperature and the cooling-air requirements.

Finally, numerical illustrations are given, both of the complete solution and of the simplified solutions where the charts can be used. These numerical results also clarify the relative values of the different terms and in many cases justify in part the omission of some.

ANALYSIS

This investigation is limited to one-dimensional spanwise blade-temperature distributions through air-cooled blades having the three different general air-passage configurations, as shown in figure 1. Because of this restriction to spanwise investigations, application of the temperature-distribution equations that are derived herein is also limited. For metals with low thermal conductivities, such as the high-temperature alloys now in use, the results are valid for wall thicknesses not exceeding about 0.15 inch. This condition can easily be met in the central part of the blade, but cannot easily be satisfied at the leading and trailing edges of current configurations. Because the leading-edge outside heat-transfer coefficient varies as the reciprocal of the square root of the square root of the leading-edge radius, the chordwise temperature distributions must be separately investigated when the leading-edge radius is small. Use of auxiliary methods for augmenting the cooling of the leading and trailing sections must also be separately investigated. Because the temperature gradients throughout the greater part of the blade are essentially radial, knowledge of the radial temperature distribution provides a reasonably accurate indication of the blade temperatures.

An equation for the spanwise blade-metal temperature distribution is derived for an air-cooled blade with an insert, with allowance for cooling-air-temperature change due to heat transfer and rotation, radiation, and radial heat conduction. Because calculations show that some of these effects are of minor importance, simplified spanwise-temperature-distribution equations may be obtained by neglecting some of these factors. The results are presented as cases I to V, and the modifications in the equations necessary to make each applicable to hollow blades and hollow blades with internal fins are noted.

ASSUMPTIONS

In order to obtain a spanwise blade-metal temperature distribution (case I), the following assumptions are made:

1. The variations in area, perimeter, and thermal conductivity are negligible over the blade span.
2. The outside and inside heat-transfer coefficients are constant over the blade outer and inner surfaces, respectively.
3. The effective gas temperature is constant over the blade outer surface.
4. The only surfaces external to the rotor that radiate heat to the blades are the turbine nozzles.
5. The turbine nozzles are at a temperature equal to the effective gas temperature relative to the rotor blades. For cooled nozzles, this temperature is high; for uncooled nozzles, this temperature is low.
6. The radiation coefficients for nozzle, blade, and insert surfaces remain constant at mean values over the blade span.

Assumptions 1 and 2 can be eliminated only if numerical solutions are determined. Calculations that were made revealed that when the factors in assumptions 1 and 2 are permitted to vary and numerical solutions are used, very little difference in the spanwise blade-temperature distribution results. Because of these results and of the greater simplicity in the use of closed solutions, assumptions 1 and 2 are made in the investigation presented herein.

The blade-temperature distribution is sensitive to selection of the average inside heat-transfer coefficient, which in turn is dependent upon the passage configuration. For the numerical results to be given subsequently, the inside heat-transfer coefficient was determined by use of equation (4f) in reference 1 (p. 170):

$$h_i=0.020\left(\frac{D_h G_a}{\mu_a}\right)^{0.8}\frac{k_a}{D_h}$$

where the hydraulic diameter D_h is given by

$$D_h=\frac{4A_c}{l_c}$$

(All symbols are defined in appendix A.) By neglecting changes in h_i due to variations in μ_a and k_a and incorporating the values of μ_a and k_a in the constant,

$$h_i=\frac{0.00288}{A_c}(l_c)^{0.2}(w_a)^{0.8}$$

This form is used in the calculations. Here the total wetted perimeter l_c and the total inside flow area A_c vary with the coolant-passage configurations.

Calculations revealed that slight variations in effective gas temperature result in even smaller variations in the spanwise blade-temperature distributions. For large variations in effective gas temperature, assumption 3 can be removed and a general solution for the temperature distribution including a change in effective gas temperature can be obtained. Such a solution is given in a later section of this report.

BLADE-TEMPERATURE-DISTRIBUTION EQUATIONS

Case I.—Case I includes cooling-air-temperature change due to heat transfer and rotation, radiation, and radial heat conduction.

1. *Insert blade.*—A sketch of an air-cooled hollow blade with an insert is given in figure 2. The directions of heat

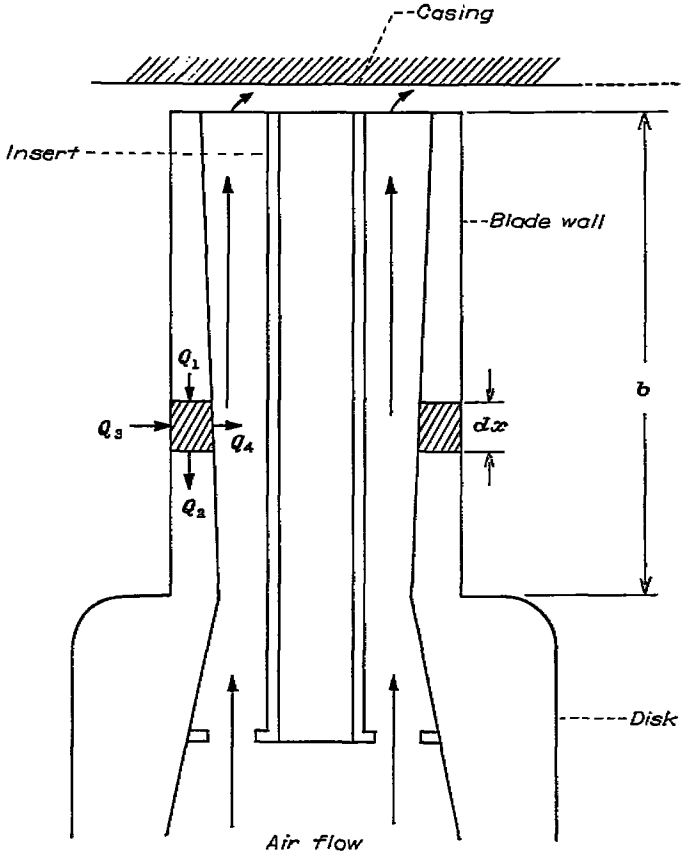

FIGURE 2.—Heat flow in air-cooled turbine blade with insert.

flow in a section of the blade are shown. A heat balance for this section is set up (appendix B), which reduces to

$$k_B l_{B,as} \tau_{B,as} \frac{d^2T_B}{dx^2}+(h_N L_e+h_s l_o)(T_{g,e}-T_B)= h_i l_i(T_B-T_{a,e})+h_s l_i(T_B-T_s) \quad (1)$$

if it is assumed that no temperature gradient exists in the insert. The following expression for the change in the cooling-air temperature is obtained by differentiation of the expression for $T_{a,e}$ obtainable from equation (1) (appendix B, equation (B2)):

$$\frac{dT_{a,e}}{dx}=-\frac{1}{G_2}\frac{d^3T_B}{dx^3}+\frac{1}{G_2}(G_1+G_2+G_3)\frac{dT_B}{dx} \quad (2)$$

where

$$G_1=\frac{h_s l_i}{k_B l_{B,as} \tau_{B,w}}$$

$$G_2=\frac{h_i l_i}{k_B l_{B,as} \tau_{B,w}}$$

$$G_3=\frac{h_N L_e+h_s l_o}{k_B l_{B,as} \tau_{B,w}}$$

A second expression for the change in cooling-air temperature is obtained by adding the changes due to the heat transferred by the blade and due to compression in the blade (appendix B):

$$\frac{dT_{a,e}}{dx}=\frac{h_i l_i}{c_p w_a}T_B-\frac{h_i(l_i+l_s)}{c_p w_a}T_{a,e}+\frac{h_i l_s}{c_p w_a}T_s+\frac{\omega^2(r_r+x)}{gJc_p} \quad (3)$$

Substitution of the value of $T_{a,e}$, obtained by solving equation (1), into equation (3) and equating the result to equation (2) gives the blade-temperature-distribution equation

$$\frac{d^3T_B}{dx^3}+Y_1\frac{d^2T_B}{dx^2}-(G_1+G_2+G_3)\frac{dT_B}{dx}+ \left[\frac{h_i l_i}{c_p w_a}G_2-Y_1(G_1+G_2+G_3)\right]T_B=-\frac{\omega^2 G_2}{gJc_p}x- \left[\frac{\omega^2 G_2}{gJc_p}r_r+\left(\frac{h_i l_s}{c_p w_a}G_2+Y_1 G_1\right)T_s+Y_1 G_3 T_{g,e}\right] \quad (4)$$

where

$$Y_1=\frac{h_i(l_i+l_s)}{c_p w_a}$$

For any chosen set of turbine operating conditions, the coefficients in all terms in equation (4) are constants, and equation (4) is a third-order ordinary linear differential equation with constant coefficients. The method of solution is standard. (See reference 2.)

The general solution to equation (4) contains three integration constants, and three boundary conditions are therefore needed in order to evaluate these constants. The boundary conditions are obtained by assuming a blade-root cooling-air temperature, a blade-root metal temperature, and a vanishing metal-temperature gradient at the blade tip.

2. *Hollow blade.*—Equation (4), as previously stated, was obtained for a blade with an insert; however, with slight alterations, it may also be applied to hollow blades and hollow blades with internal cooling fins. For a hollow blade, h_s and l_s vanish. As a result, the value of Y_1 is altered and G_1 and the coefficient of T_s vanish. The following equation to be used for a hollow blade results from the modification of equation (4) by these minor changes:

$$\frac{d^3T_B}{dx^3}+\frac{h_i l_i}{c_p w_a}\frac{d^2T_B}{dx^2}-(G_2+G_3)\frac{dT_B}{dx}-\frac{h_i l_i}{c_p w_a}G_3 T_B =-\frac{\omega^2 G_2}{gJc_p}x-\left(\frac{\omega^2 G_2}{gJc_p}r_r+\frac{h_i l_i}{c_p w_a}G_3 T_{g,e}\right) \quad (5)$$

3. *Finned blade.*—More extensive changes are necessary for application of equation (4) to a finned blade. In addition to the changes noted for a hollow blade, alterations are required in the area affected by conduction and in the inside heat-transfer coefficient in order to account for the effects of the fins. For radial conduction, the area $l_{B,av}\tau_{B,w}$ is replaced by $l_{B,av}\tau_{B,w}+2L_f\tau_f F$ for a finned blade (provided the fins are attached to the rim), where L_f is the effective fin width from blade wall to mean camber line, τ_f is the fin thickness, and F is the number of fins.

For a finned blade, an inside heat-transfer coefficient based on the total heat-transfer surface area and on the blade-wall and fin temperatures can be obtained. It is convenient, however, to determine an over-all inside heat-transfer coefficient for a finned blade based only on wall temperature and wall-surface area. The following relation, originally derived for finned flat plates (reference 3) and experimentally verified for finned flat plates and finned cylinders, is used:

$$h_f=\frac{h_i}{m+\tau_f}\left(\frac{2\tanh\phi_f L_f}{\phi_f}+m\right) \tag{6}$$

where m is the average fin spacing and

$$\phi_f=\sqrt{\frac{2h_i}{k_B\tau_f}}$$

To summarize, when equation (4) is applied to a finned blade, the value of Y_1 is altered, G_1 and the coefficient of T_s vanish, the values of G_2 and G_3 are altered, and h_i is replaced by h_f, which is obtained as previously explained. The following equation to be used for a finned blade results from the modification of equation (4) by these changes:

$$\frac{d^3T_B}{dx^3}+\frac{h_f l_i}{c_p w_a}\frac{d^2T_B}{dx^2}-(G_2'+G_3')\frac{dT_B}{dx}-\frac{h_f l_i}{c_p w_a}G_3'T_B$$
$$=-\frac{\omega^2 G_2'}{gJc_p}x-\left(\frac{\omega^2 G_2'}{gJc_p}r_r+\frac{h_f l_i}{c_p w_a}G_3'T_{g,e}\right) \tag{7}$$

where

$$G_2'=\frac{h_f l_i}{k_B(l_{B,av}\tau_{B,w}+2L_f\tau_f F)}$$

and

$$G_3'=\frac{h_N L_e+h_o l_o}{k_B(l_{B,av}\tau_{B,w}+2L_f\tau_f F)}$$

(For fins not attached to the rim, G_2' and G_3' are replaced by G_2 and G_3.)

Case II.—Case II includes cooling-air-temperature change due to heat transfer and rotation and radiation (neglects radial conduction).

The parameter that measures the relative importance of conduction to the rim is (reference 4)

$$\zeta=(r-r_r)\sqrt{\frac{h_o l_o+h_i l_i}{k_B A_{B,w}}}$$

The spanwise blade-metal temperature distributions for certain air-cooled hollow blades that have been studied indicate that conduction to the rim is negligible beyond a point 0.8 inch from the rim. The value of ζ at this point is between 3 and 4. For the air-cooled hollow blade of reference 5, the value of ζ for negligible conduction to the rim is 3.4 and occurs at a point 10 percent of the blade span from the root (0.4 in.). Equation (10) of reference 1 (p. 232) indicates that when ζ is equal to or greater than 4, the temperature difference between the combustion gas and the blade metal is changed less than 1.8 percent by conduction to the rim. Conduction can therefore be neglected for values of ζ equal to or greater than 3.5.

1. *Insert blade.*—When radial conduction is neglected, the heat-balance equation (1) reduces to

$$(h_N L_e+h_o l_o)(T_{g,e}-T_B)=h_i l_i(T_B-T_{a,e})+h_s l_i(T_B-T_s) \tag{8}$$

From equation (8) it is found that

$$T_{a,e}=\frac{T_B}{Y_2}-\frac{h_s l_i}{h_i l_i}T_s-\frac{h_N L_e+h_o l_o}{h_i l_i}T_{g,e} \tag{9}$$

where

$$Y_2=\frac{h_i l_i}{h_N L_e+h_o l_o+h_i l_i+h_s l_i}$$

Then

$$\frac{dT_{a,e}}{dx}=\frac{1}{Y_2}\frac{dT_B}{dx} \tag{10}$$

When equations (3) and (10) are equated and equation (9) is used, the following expression results:

$$\frac{dT_B}{dx}+\left(Y_1-\frac{h_i l_i}{c_p w_a}Y_2\right)T_B=\frac{\omega^2 x}{gJc_p}Y_2+$$
$$\frac{\omega^2 r}{gJc_p}+\left[\frac{h_N L_e+h_o l_o}{h_i l_i}Y_1 T_{g,e}+\left(\frac{h_s}{h_i}Y_1+\frac{h_i l_i}{c_p w_a}\right)T_s\right]Y_2 \tag{11}$$

For any chosen set of turbine operating conditions, equation (11) reduces to a first-order linear differential equation with constant coefficients. The single integration constant may be evaluated from an assumed cooling-air temperature at the blade root.

2. *Hollow blade.*—Equation (11) is applicable to hollow air-cooled blades when alterations in Y_1 and Y_2 are made; these alterations result from the vanishing of both h_s and l_s. The resulting equation for a hollow blade is

$$\frac{dT_B}{dx}+\frac{h_i l_i}{c_p w_a}(1-Y_2')T_B=\frac{\omega^2 x}{gJc_p}Y_2'+\left(\frac{\omega^2 r_r}{gJc_p}+\frac{h_N L_e+h_o l_o}{c_p w_a}T_{g,e}\right)Y_2' \tag{12}$$

where

$$Y_2'=\frac{h_i l_i}{h_N L_e+h_o l_o+h_i l_i}$$

3. *Finned blades.*—Equation (11) can be applied to a finned blade if, in addition to the alterations made for application

to a hollow blade, the inside heat-transfer coefficient h_f is used. For a finned blade, equation (11) becomes

$$\frac{dT_B}{dx}+\frac{h_f l_i}{c_p w_a}(1-Y_2'')\,T_B=\frac{\omega^2 x}{gJc_p}\,Y_2''+\left(\frac{\omega^2 r_r}{gJc_p}+\frac{h_N L_e+h_o l_o}{c_p w_a}T_{g,e}\right)Y_2'' \tag{13}$$

where

$$Y_2''=\frac{h_f l_i}{h_N L_e+h_o l_o+h_f l_i}$$

Case III.—Case III includes cooling-air-temperature change due to heat transfer and rotation (neglects radiation and radial conduction).

Equation (11) is applicable if insert and nozzle radiation, in addition to radial conduction, are neglected. Calculations that are discussed in a later section of this report revealed that results obtained by use of equations (4) and (11) with radiation neglected agreed very closely; as a result of the greater simplicity, use of equation (11) is recommended when conditions permit. According to a previous investigation, radiation effects may be neglected without sizable error for stator temperatures as high as 3000° F. Also, neglecting insert radiation results in no heat transfer between the insert and the cooling air. As a consequence, equation (3) reduces to

$$\frac{dT_{a,e}}{dx}=\frac{h_i l_i}{c_p w_a}(T_B-T_{a,e})+\frac{\omega^2(r_r+x)}{gJc_p} \tag{14}$$

The heat-balance equation for this case is

$$h_o l_o(T_{g,e}-T_B)=h_i l_i(T_B-T_{a,e}) \tag{15}$$

Equation (15) is solved for $T_{a,e}$ and $dT_{a,e}/dx$ is obtained. This result is equated to equation (14) with the value of $T_{a,e}$ inserted. The result is

$$\frac{dT_B}{dx}+\frac{h_o l_o}{c_p w_a(1+\lambda)}T_B=\frac{h_o l_o}{c_p w_a(1+\lambda)}T_{g,e}+\frac{\omega^2(r_r+x)}{gJc_p(1+\lambda)} \tag{16}$$

where

$$\lambda=\frac{h_o l_o}{h_i l_i}$$

A solution of equation (16) is

$$T_B=T_{g,e}+\frac{\omega^2 w_a(r_r+x)}{gJh_o l_o}+C_1 e^{-\frac{h_o l_o x}{c_p w_a(1+\lambda)}}-\frac{\omega^2 w_a^2 c_p(1+\lambda)}{gJh_o^2 l_o^2} \tag{17}$$

The integration constant C_1 can be evaluated by substitution of equation (17) into equation (15) and application of the boundary condition

$$T_{a,e}=T_{a,e,r}$$

when

$$x=0$$

It is found that

$$C_1=\frac{c_p\omega^2 w_a^2(1+\lambda)}{gJh_o^2 l_o^2}-\frac{\omega^2 r_r w_a}{gJh_o l_o}-\frac{T_{g,e}-T_{a,e,r}}{1+\lambda}$$

The result of the substitution of this expression for C_1 into equation (17) and of simplification leads to the nondimensional blade-temperature distribution

$$\frac{T_{g,e}-T_B}{T_{g,e}-T_{a,e,r}}=\frac{1}{1+\lambda}e^{-\left(\frac{1}{1+\lambda}\frac{h_o l_o b}{c_p w_a}\frac{x}{b}\right)}-\frac{\omega^2 w_a b}{gJh_o l_o(T_{g,e}-T_{a,e,r})}\frac{x}{b}+\left[1-e^{-\left(\frac{1}{1+\lambda}\frac{h_o l_o b}{c_p w_a}\frac{x}{b}\right)}\right]\left[\frac{\omega^2 w_a}{gJh_o l_o(T_{g,e}-T_{a,e,r})}\right]\left[\frac{c_p w_a(1+\lambda)}{h_o l_o}-r_r\right] \tag{18}$$

It is possible to remove the restriction that $T_{g,e}$ be constant and to solve equation (16) for the blade-metal temperature for a varying $T_{g,e}$. A more general solution then results from equation (16) and is given as follows:

$$T_B=e^{-\frac{h_o l_o x}{c_p w_a(1+\lambda)}}\frac{h_o l_o}{c_p w_a(1+\lambda)}\int_0^b T_{g,e}\,e^{\frac{h_o l_o x}{c_p w_a(1+\lambda)}}\,dx+\frac{\omega^2 w_a(r_r+x)}{gJh_o l_o}+C_2 e^{-\frac{h_o l_o x}{c_p w_a(1+\lambda)}}-\frac{\omega^2 w_a^2 c_p(1+\lambda)}{gJh_o^2 l_o^2} \tag{19}$$

The integration constant C_2 can be evaluated in the same way that the value of the constant C_1 in equation (17) is obtained.

Case IV.—Case IV includes cooling-air-temperature change due to heat transfer from the blade only.

In several numerical calculations, some of which are discussed in a later section, the predominant term in the evaluation of the temperature ratio $\frac{T_{g,e}-T_B}{T_{g,e}-T_{a,e,r}}$ is the exponential term, and the other two terms are of minor importance. This generalization is particularly true for finned blades, as is shown, because the insertion of fins into blades decreases the flow area and at the same time increases the heat-transfer surface area; an increased value of h_i, hence a smaller value of λ, and a greater predominance of the exponential term are thus obtained. For this reason, it is desirable to know the temperature-distribution equation, including the change in cooling-air temperature due to heat transfer from the blades only.

The blade-temperature distribution for this case can be obtained by setting $\omega=0$ in equation (18); that is,

$$\frac{T_{g,e}-T_B}{T_{g,e}-T_{a,e,r}}=\frac{1}{1+\lambda}e^{-\left(\frac{1}{1+\lambda}\frac{h_o l_o b}{c_p w_a}\frac{x}{b}\right)} \tag{20}$$

Case V.—Case V includes the average cooling-air temperature. In several available correlation equations (reference 6) used for obtaining values of the inside heat-transfer coefficient, fluid properties are based on blade temperature. In order to obtain a first approximation of blade temperatures preparatory to the calculation of h_i, it is desirable to

have as simple an equation for average blade temperature as possible. Equation (21), which follows, gives an average blade temperature and is well suited for this purpose.

If an average cooling-air temperature is assumed, an average blade temperature for an air-cooled blade can be immediately determined by the solution of equation (15):

$$T_{B,av}=\frac{T_{a,e,av}+\lambda T_{g,e}}{1+\lambda} \qquad (21)$$

If each member of equation (21) is subtracted from $T_{g,e}$, the following nondimensional equation is obtained:

$$\frac{T_{g,e}-T_{B,av}}{T_{g,e}-T_{a,e,av}}=\frac{1}{1+\lambda} \qquad (22)$$

COOLING-AIR REQUIREMENTS

In order to determine the cooling-air requirements for the various blade configurations, the blade-temperature-distribution equations just presented in cases I to V must be used and, in addition, calculation of allowable blade-temperature distributions must be possible. Allowable blade-temperature distributions, dependent on the kind of blade material and type of blade configuration considered, can be obtained from blade-stress calculations and blade-failure criterions. Centrifugal, bending, thermal, and vibratory stresses are all present in a turbine blade in operation. Rupture, creep, and endurance limits are the primary failure criterions.

Present knowledge of the magnitudes and the concentrations of the various stresses in a blade and of the predominant blade-failure criterion is very limited; as a consequence, it is necessary for a general analysis to approximate the allowable blade-temperature distribution in the best way possible.

This approximation has consisted of the consideration of centrifugal stress and stress-rupture data only. Some allowance for stresses other than centrifugal is made possible by the introduction of a safety factor; one such safety factor is introduced if an allowable blade life in excess of that desired is assumed. For an assumed blade material, configuration, allowable life, and tip speed, the allowable blade-temperature distribution has been calculated in the following way:

A radial stress distribution is obtained for the assumed blade configuration and tip speed. From a cross plot of available stress-rupture data for the assumed blade material and blade life and the calculated radial stress distribution through the blade, it is possible to determine the maximum permissible spanwise temperature through the blade.

If the actual and allowable blade-temperature distributions for the same tip speed are obtained and plotted on the same coordinates, the maximum allowable effective gas temperature for this tip speed can be determined. This maximum is determined when the actual blade-temperature-distribution curve has a point of tangency with the allowable-temperature curve (fig. 3). Blade stresses above the allowable limit prevail in the section of a blade that corresponds to any region of overlapping of the actual and allowable-blade-temperature curves. The curves may also be used to determine the maximum tip speed for a given calculated temperature distribution.

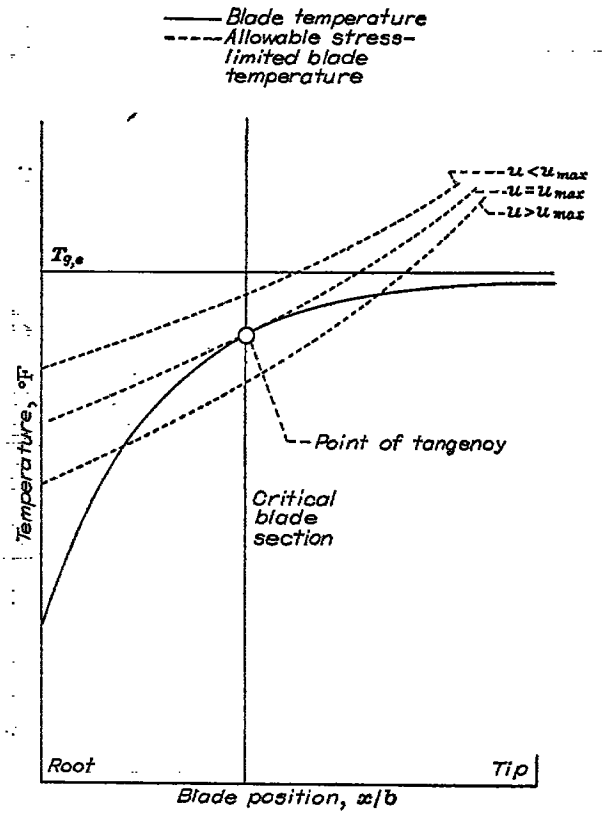

FIGURE 3.—Method of determining limiting speed and critical blade section from curves of temperature distribution and allowable stress-limited blade temperature.

If an effective gas temperature is assumed, blade-temperature distributions for various cooling-air ratios may be determined, and the distribution that matches the allowable blade-temperature distribution then determines the cooling-air requirement for the blade under consideration.

NONDIMENSIONAL CHARTS

Because the results of numerical calculations (such as the examples hereinafter presented) revealed that the effects of radial heat conduction are negligible except in the immediate vicinity of the blade root and that the effects of neglecting both radial conduction and radiation are also small, no general solutions are obtained for the differential equations involving these quantities. The first general solution that is obtained for air cooling involves cooling-air-temperature change due to heat transfer and rotation; this solution is given by

$$\frac{T_{g,e}-T_B}{T_{g,e}-T_{a,e,r}}=\frac{1}{1+\lambda}e^{-\left(\frac{1}{1+\lambda}\frac{h_o l_o b}{c_p w_a}\frac{r}{b}\right)}-\frac{\omega^2 w_a b}{gJh_o l_o(T_{g,e}-T_{a,e,r})}\frac{x}{b}+\left[1-e^{-\left(\frac{1}{1+\lambda}\frac{h_o l_o b}{c_p w_a}\frac{x}{b}\right)}\right]\left[\frac{\omega^2 w_a}{gJh_o l_o(T_{g,e}-T_{a,e,r})}\right]\left[\frac{c_p w_a(1+\lambda)}{h_o l_o}-r_r\right] \qquad (18)$$

For any given turbine and set of turbine operating conditions, the spanwise temperature distribution through the air-cooled blades may be determined by use of figure 4 and

a simple calculation. Figure 4(a) serves to evaluate the first term in the right member of equation (18). For the given conditions, values of the outside and inside heat-transfer coefficients and values of the effective gas temperature and the effective cooling-air temperature at the blade root can be obtained. The abscissa in quadrant I represents $\frac{h_o l_o b}{c_p w_a}$, and a family of curves for various values of x/b in quadrant I immediately determines the values of $\frac{h_o l_o b}{c_p w_a}\frac{x}{b}$, represented as the ordinate in quadrants I and II. A family of curves in quadrant II for values of $\frac{1}{1+\lambda}$ determines values of $\frac{h_o l_o b}{c_p w_a}\frac{x}{b}\frac{1}{1+\lambda}$ as the abscissa in quadrants II and III. The exponential curve in quadrant III determines the values of the exponential function as the ordinates of quadrants III and IV. Another family of curves (like those in quadrant II) for values of $\frac{1}{1+\lambda}$ then determines, as the abscissa in quadrant IV, the value of the first term in the right member of equation (18).

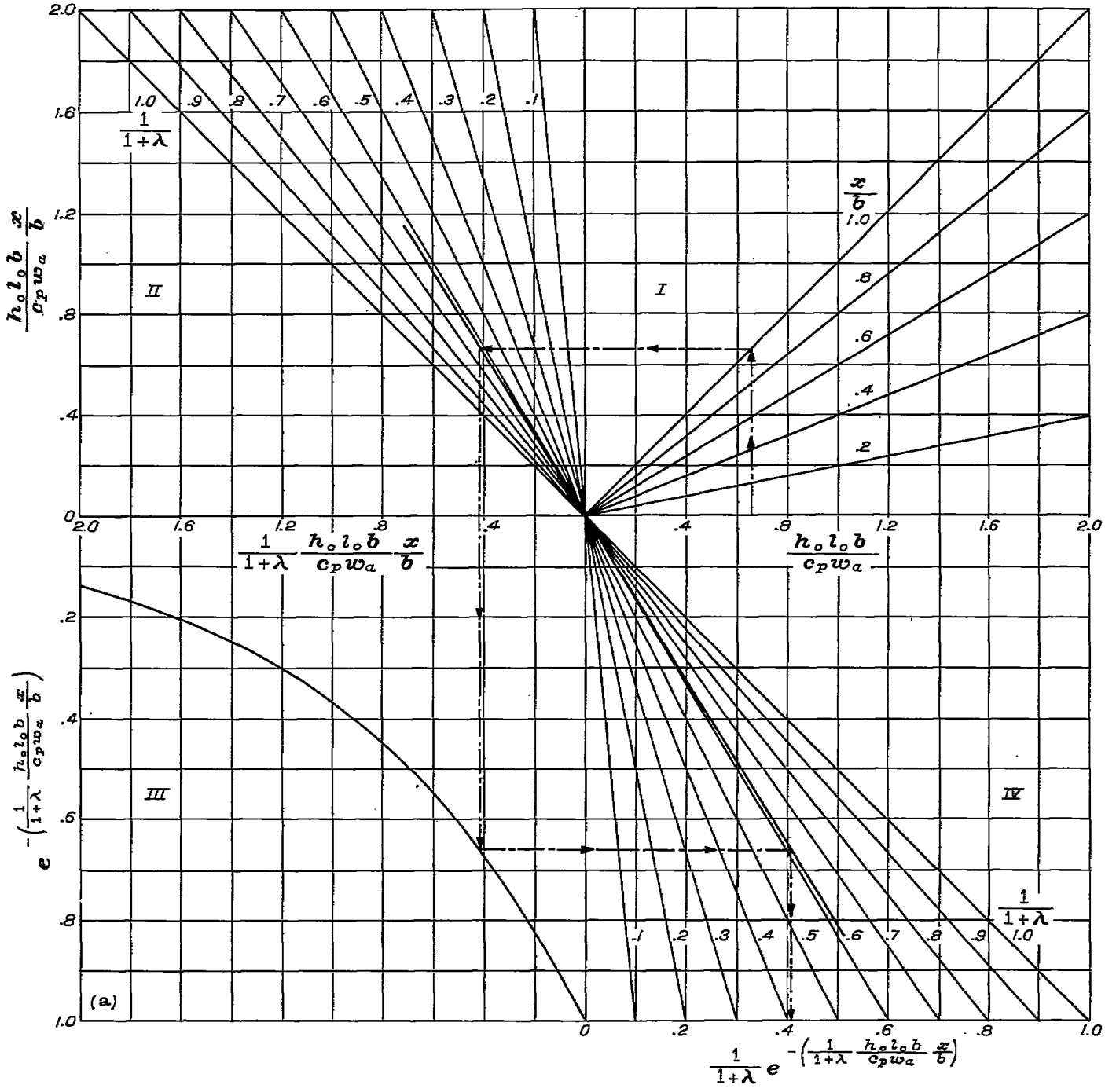

(a) Includes cooling-air-temperature change due to heat transfer but neglects rotation, radiation, and radial conduction. (A 21- by 22-in. print of this chart is available upon request from NACA.)

FIGURE 4.—Chart for calculation of spanwise temperature distribution through air-cooled turbine blade.

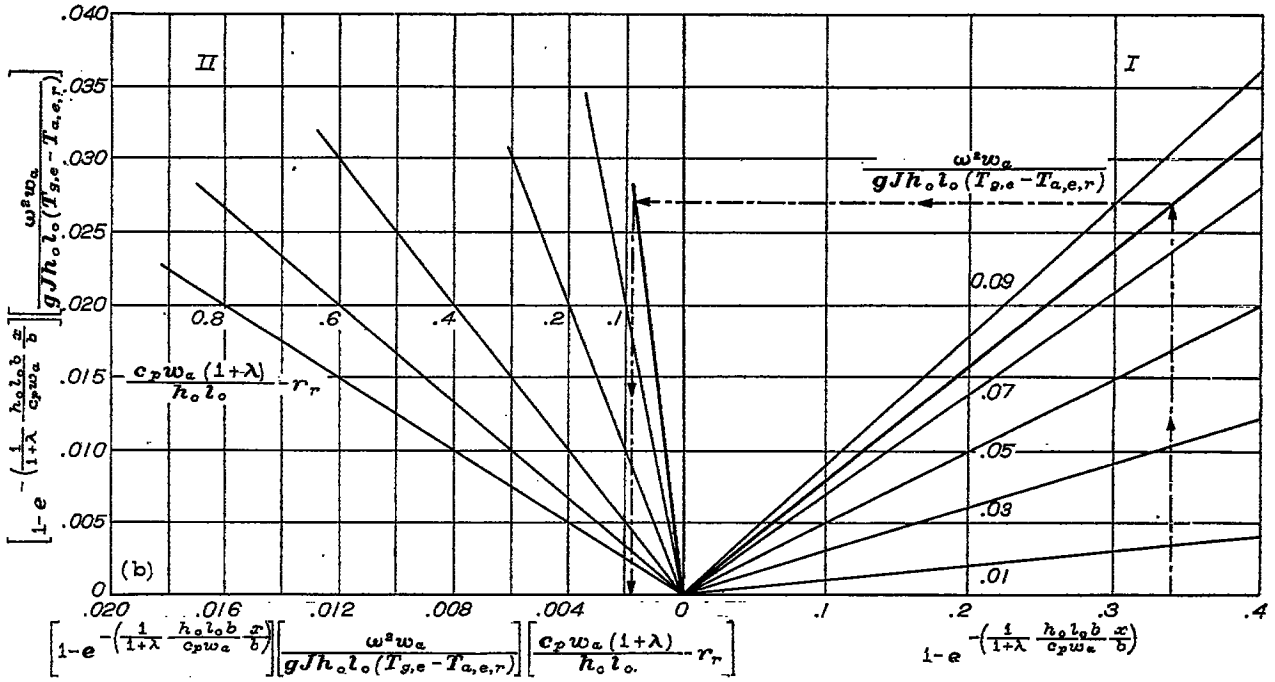

(b) Includes cooling-air-temperature change due to heat transfer and part of effect of rotation. (A 22- by 13-in. print of this chart is available upon request from NACA.)

FIGURE 4.—Concluded.

Calculation of the third term in the right member of equation (18) can be made with figure 4(b). For any desired blade position, the values of the exponential function were found as the ordinates in quadrant III of figure 4(a). These values, subtracted from 1, form the abscissa in quadrant I of figure 4(b). A family of curves in quadrant I for various values of $\frac{\omega^2 w_a}{gJh_o l_o(T_{g,e}-T_{a,e,r})}$ determines as the ordinate the values of

$$\left[1-e^{-\left(\frac{1}{1+\lambda}\frac{h_o l_o b}{c_p w_a}\frac{x}{b}\right)}\right]\left[\frac{\omega^2 w_a}{gJh_o l_o(T_{g,e}-T_{a,e,r})}\right]$$

Another family of curves, in quadrant II, for values of $\frac{c_p w_a(1+\lambda)}{h_o l_o}-r_r$ determines, as the abscissa of quadrant II, the value of the third term in the right member of equation (18).

The parameter $\frac{\omega^2 w_a}{gJh_o l_o(T_{g,e}-T_{a,e,r})}$, multiplied by the appropriate value of x, then yields the value of the second term in the right member of equation (18).

Combination of the three right-member contributions yields the desired temperature ratio at any blade position, and several repetitions for different blade positions will result in the desired blade-temperature distribution.

If rotational effects are neglected, the right member of equation (18) reduces to the first term; that is,

$$\frac{T_{g,e}-T_B}{T_{g,e}-T_{a,e,r}}=\frac{1}{1+\lambda}e^{-\left(\frac{1}{1+\lambda}\frac{h_o l_o b}{c_p w_a}\frac{x}{b}\right)} \tag{20}$$

and the temperature distribution through the air-cooled blade can be found by use of figure 4(a).

If in addition to neglecting effects of rotation, an average cooling-air temperature is considered, the temperature-distribution equation reduces to

$$\frac{T_{g,e}-T_{B,av}}{T_{g,e}-T_{a,e,av}}=\frac{1}{1+\lambda} \tag{22}$$

For a given turbine and set of turbine operating conditions, calculations of the heat-transfer coefficients and of the effective gas temperature and effective cooling-air temperature at the blade root may be made. With these temperatures and the inner- and outer-blade perimeters, the desired temperature ratio can be determined from figure 5, which contains a plot of $\frac{T_{g,e}-T_{B,av}}{T_{g,e}-T_{a,e,av}}$ against λ.

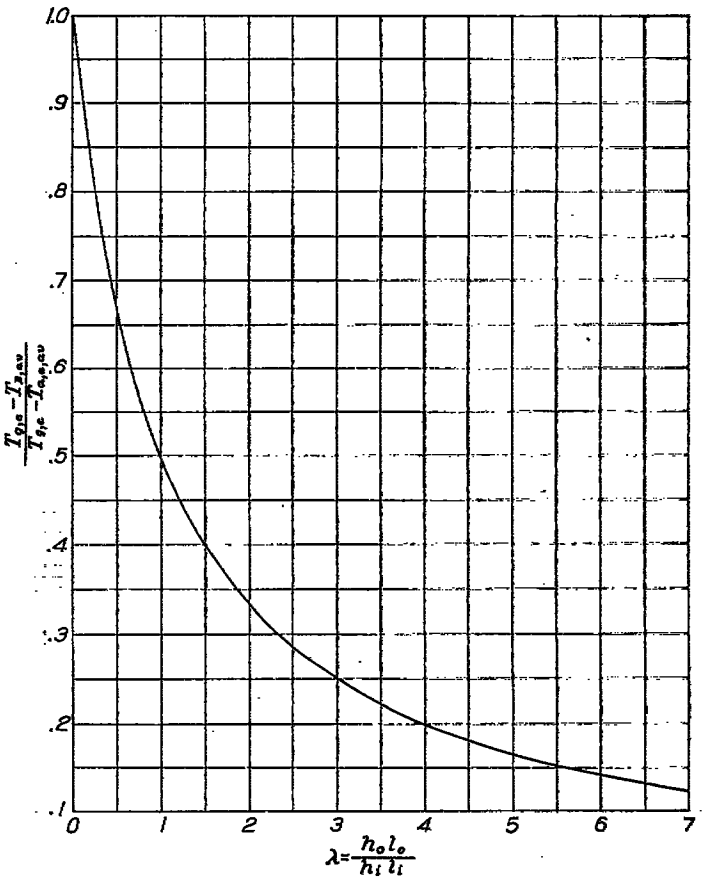

FIGURE 5.—Chart for calculation of spanwise temperature distribution through air-cooled turbine blade for average cooling-air temperature.

ILLUSTRATIVE EXAMPLES

In order to illustrate the use of some of the analytical results previously presented and to determine the magnitudes of some of the quantities contained in the analytical equations, several numerical results are given. A turbine blade was selected having an external shape similar to that of the rotor-root section of a conventional gas-turbine design (fig. 1). Numerical values used in the calculations are as follows:

TURBINE-BLADE DIMENSIONS

Number of blades	54
Blade height, b, ft	0.333
Blade outer perimeter, l_o, ft	0.385
Blade inner perimeter, l_i, ft	0.314
Perimeter of insert, l_s, ft	0.313
Perimeter of cooling passages for finned blade, l_c, ft	1.070
External cross-sectional blade area, A_B, sq ft	0.00424
Area of cooling-air passage, A_c, sq ft	
Hollow blade	0.00241
Insert blade	0.00100
Finned blade	0.00147
Blade-tip radius, r_T, ft	1.083
Blade-wall thickness, $\tau_{B,w}$, ft	0.005
Effective blade width, L_e, ft	0.1065
Effective fin width, L_f, ft	0.009
Fin spacing, m, ft	0.0035
Fin thickness, τ_f, ft	0.0017

CONDITIONS FOR NUMERICAL EXAMPLE

Hot-gas flow per blade, w_g	
lb/hr	5260
lb/sec	5260/3600
Cooling-air flow per blade, w_a	
lb/hr	coolant-flow ratio×5260
lb/sec	coolant-flow ratio×5260/3600
Outside heat-transfer coefficient, h_o	
Btu/(hr)(°F)(sq ft)	198
Btu/(sec)(°F)(sq ft)	198/3600
Cooling-air temperature at blade root, $T_{a,c,r}$, °F	400
Effective hot-gas temperature, $T_{g,e}$, °F	1700–1900
Average insert temperature, T_s, °F	700
Radiation coefficient from nozzle to blade wall for $T_{g,e}$=1700° F, h_N	
Btu/(hr)(°F)(sq ft)	43
Btu/(sec)(°F)(sq ft)	43/3600
Radiation coefficient from nozzle to blade wall for $T_{g,e}$=1900° F, h_N	
Btu/(hr)(°F)(sq ft)	56
Btu/(sec)(°F)(sq ft)	56/3600
Radiation coefficient from blade wall to insert surface, h_s	
Btu/(hr)(°F)(sq ft)	12
Btu/(sec)(°F)(sq ft)	12/3600
Nozzle-surface emissivity	0.95
Insert-surface emissivity	0.50
Blade-wall emissivity at average T_B=1400° F	0.90
Rotative speed, radians/sec	1200
Tip speed, u, ft/sec	1300
Specific heat of cooling air, Btu/(lb)(°F)	0.241
Blade thermal conductivity,	
Btu/(hr)(°F)(ft)	12
Btu/(sec)(°F)(ft)	12/3600

SOLUTION OF GENERAL CASE, CASE I

The first temperature distribution obtained is for the insert blade and includes the cooling-air-temperature change due to heat transfer and rotation, radiation, and radial heat conduction; that is, equation (4) is used. An effective gas temperature of 1900° F, a blade-root cooling-air temperature of 400° F, an average insert temperature of 700° F, and a ratio of coolant flow to gas flow (coolant-flow ratio) of 0.03 are assumed. From the values given in the two preceding tables, the coefficients in the differential equation are determined as follows:

$$h_i=\frac{0.00288(l_i+l_s)^{0.2}w_a^{0.8}}{A_c}$$

$$=\frac{0.00288(0.314+0.313)^{0.2}[(0.03)(5260)]^{0.8}}{0.00100}$$

$$=151 \text{ Btu/(hr) (°F) (sq ft)}$$

$$=151/3600 \text{ Btu/(sec) (°F) (sq ft)}$$

$$Y_1=\frac{h_i(l_i+l_s)}{c_p w_a}$$

$$=\frac{151\ (0.314+0.313)\ 3600}{3600\ (0.241)\ (158)}$$

$$=2.484 \text{ (ft)}^{-1}$$

$$G_1=\frac{h_s l_i}{k_B l_{B,a} \tau_{B,w}}$$

$$=\frac{(3600)\ (12)\ (0.314)}{(3600)\ (12)\ (0.350)\ (0.005)}$$

$$=179.4 \text{ (ft)}^{-2}$$

$$G_2=\frac{h_i l_i}{k_B l_{B,a} \tau_{B,w}}$$

$$=\frac{(3600)\ (151)\ (0.314)}{(3600)\ (12)\ (0.350)\ (0.005)}$$

$$=2258 \text{ (ft)}^{-2}$$

$$G_3=\frac{h_N L_e+h_o l_o}{k_B l_{B,a} \tau_{B,w}}$$

$$=\frac{[(56)\ (0.1065)+(198)\ (0.385)]\ 3600}{(3600)\ (12)\ (0.350)\ (0.005)}$$

$$=3914 \text{ (ft)}^{-2}$$

$$G_1+G_2+G_3=(179.4+2258+3914)=6351 \text{ (ft)}^{-2}$$

$$\frac{h_i l_i}{c_p w_a}=\frac{(3600)\ (151)\ (0.314)}{(3600)\ (0.241)\ (158)}=1.245 \text{ (ft)}^{-1}$$

$$\frac{h_i l_i}{c_p w_a} G_2=(1.245)\ (2258)=2811 \text{ (ft)}^{-3}$$

$$Y_1(G_1+G_2+G_3)=(2.484)\ (6351)=15{,}780 \text{ (ft)}^{-3}$$

$$\frac{h_i l_i}{c_p w_a} G_2-Y_1(G_1+G_2+G_3)=2811-15{,}780$$

$$=-12{,}970 \text{ (ft)}^{-3}$$

$$\frac{\omega^2 G_2}{gJc_p}=\frac{(1200)^2\ (2258)}{(32.2)\ (778)\ (0.241)}=538{,}500° \text{ F/(ft)}^4$$

$$\frac{\omega^2 G_2}{gJc_p} r_r = (538{,}500)(0.75) = 403{,}900^\circ \text{ F/(ft)}^3$$

$$\frac{h_i l_s}{c_p w_a} G_2 = \frac{(3600)(151)(0.313)(2258)}{(0.241)(158)(3600)} = 2805 \text{ (ft)}^{-3}$$

$$Y_1 G_1 = (2.484)(179.4) = 445.8 \text{ (ft)}^{-3}$$

$$\left(\frac{h_i l_s}{c_p w_a} G_2 + Y_1 G_1\right) T_s = (2805 + 445.8)\, 700$$

$$= 2{,}276{,}000^\circ \text{ F/(ft)}^3$$

$$Y_1 G_3 T_{g,e} = (2.484)(3914)(1900) = 18{,}480{,}000^\circ \text{ F/(ft)}^3$$

The differential equation (4) then becomes

$$\frac{d^3 T_B}{dx^3} + 2.484 \frac{d^2 T_B}{dx^2} - 6351 \frac{dT_B}{dx} - 12{,}970 T_B = -538{,}500x - 21{,}160{,}000 \quad (23)$$

which may be rewritten as

$$(D^3 + 2.484 D^2 - 6351 D - 12{,}970) T_B = -538{,}500x - 21{,}160{,}000 \quad (24)$$

where D denotes differentiation. The complete solution to this equation, which consists of two parts, is

$$T_B = C_3 e^{-2.041x} + C_4 e^{79.48x} + C_5 e^{-79.92x} + 41.53x + 1611 \quad (25)$$

In order to evaluate the integration constants C_3, C_4, and C_5, the following boundary conditions were applied:

$$T_B = 1200^\circ \text{ F (assumed)}; \quad x = 0$$

$$dT_B/dx = 0; \quad x = 0.333$$

$$T_{a,e,r} = 400^\circ \text{ F (assumed)}; \quad x = 0$$

The use of the second boundary condition requires differentiation of equation (25). Use of the third boundary condition requires the solution of equation (1) for $T_{a,e,r}$ (see appendix B, equation (B2)), which in turn requires knowledge of the second derivative of equation (25). From equation (25),

$$\frac{dT_B}{dx} = -2.041 C_3 e^{-2.041x} + 79.48 C_4 e^{79.48x} - 79.92 C_5 e^{-79.92x} + 41.53$$

and

$$\frac{d^2 T_B}{dx^2} = 4.168 C_3 e^{-2.041x} + 6317 C_4 e^{79.48x} + 6388 C_5 e^{-79.92x}$$

Application of the boundary conditions then yields the following three equations for C_3, C_4, and C_5:

$$1200 = C_3 + C_4 + C_5 + 1611$$

$$0 = -1.034 C_3 + (248.1)(10^{11}) C_4 + 41.53$$

$$(2258)(400) = -(4.168 C_3 + 6317 C_4 + 6388 C_5) + 6351 C_3 + 6351 C_4 + 6351 C_5 + 10{,}230{,}000 - 7{,}562{,}000$$

or

$$C_3 + C_4 + C_5 = -411$$

$$-C_3 + (239.8)(10^{11}) C_4 = -40.14$$

$$C_3 + (5.358)(10^{-3}) C_4 - (5.830)(10^{-8}) C_5 = -278.1$$

It was then found that

$$C_3 = -278.9$$

$$C_4 = -(1.330)(10^{-11})$$

$$C_5 = -132.1$$

and hence, from equation (21)

$$T_B = -278.9\, e^{-2.041x} - 1.330\,(10^{-11})\, e^{79.48x} - 132.1\, e^{-79.92x} + 41.53x + 1611$$

Finally, by substitution of various values of x, the blade-temperature distribution was determined as follows:

x	x/b	T_B, (°F)
0	0	1200
.0167	.05	1307
.0333	.1	1342
.05	.15	1359
.0666	.2	1370
.133	.4	1404
.1998	.6	1434
.2664	.8	1460
.333	1	1479

This temperature distribution is shown by the solid line (coolant-flow ratio, 0.03) in figure 6. Three other temperature distributions are also shown in figure 6 to illustrate the

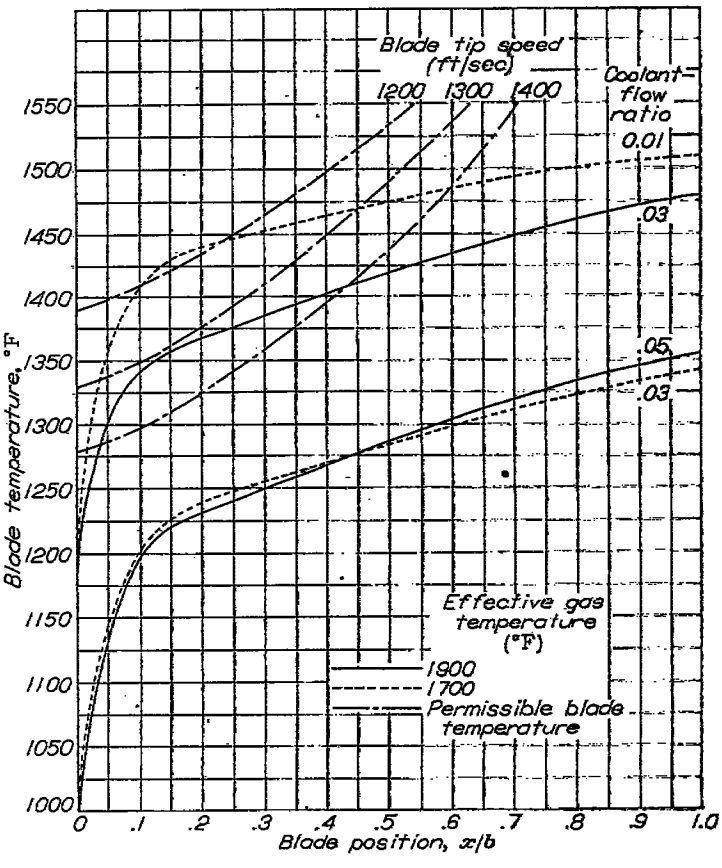

FIGURE 6.—Temperature distribution through air-cooled turbine blade with insert including change in cooling-air temperature due to heat transfer and rotation, radiation, and radial conduction. Blade-root cooling-air temperature, 400° F; average insert temperature, 700° F.

effect of a change in coolant-flow ratio and in effective gas temperature. The permissible-blade-temperature curves shown as the dashed curves were determined by cross-plotting stress-to-rupture data for S–816 for 1000-hour life and a calculated centrifugal-stress distribution through the blade.

Results of similar calculations of temperature distributions for a hollow air-cooled blade are shown in figure 7. A comparison of figures 6 and 7 shows that for an effective gas temperature of 1900° F the cooling-air requirement for the insert blade is only about one-fourth that for the hollow blade in the cases considered.

The effect of a change in blade-root temperature on the temperature distribution for the insert blade is shown in figure 8. It can be seen that no change in the temperature-distribution curve results beyond a value of x/b of about 0.23. Hence, beyond this point, radial conduction can be neglected with no error. In addition, even at the blade critical point, a change of less than 10° results from a change in blade-root temperature of 100° F. This value of 0.23 shown on figure 8 is in conformity with the previous discussion concerning the possibility of neglecting radial conduction when the parameter ζ exceeds 3.5.

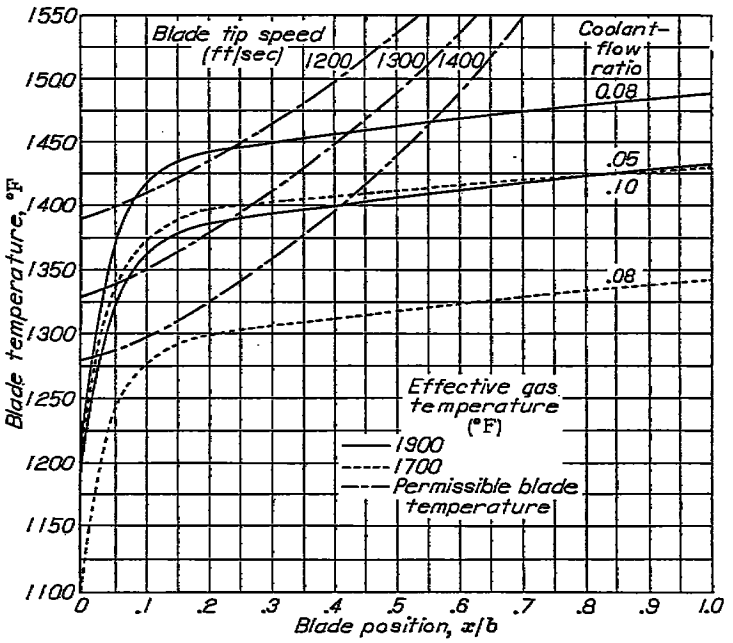

FIGURE 7.—Temperature distribution through hollow air-cooled turbine blade including change in cooling-air temperature due to heat transfer and rotation, radiation, and radial conduction. Blade-root cooling-air temperature, 400° F.

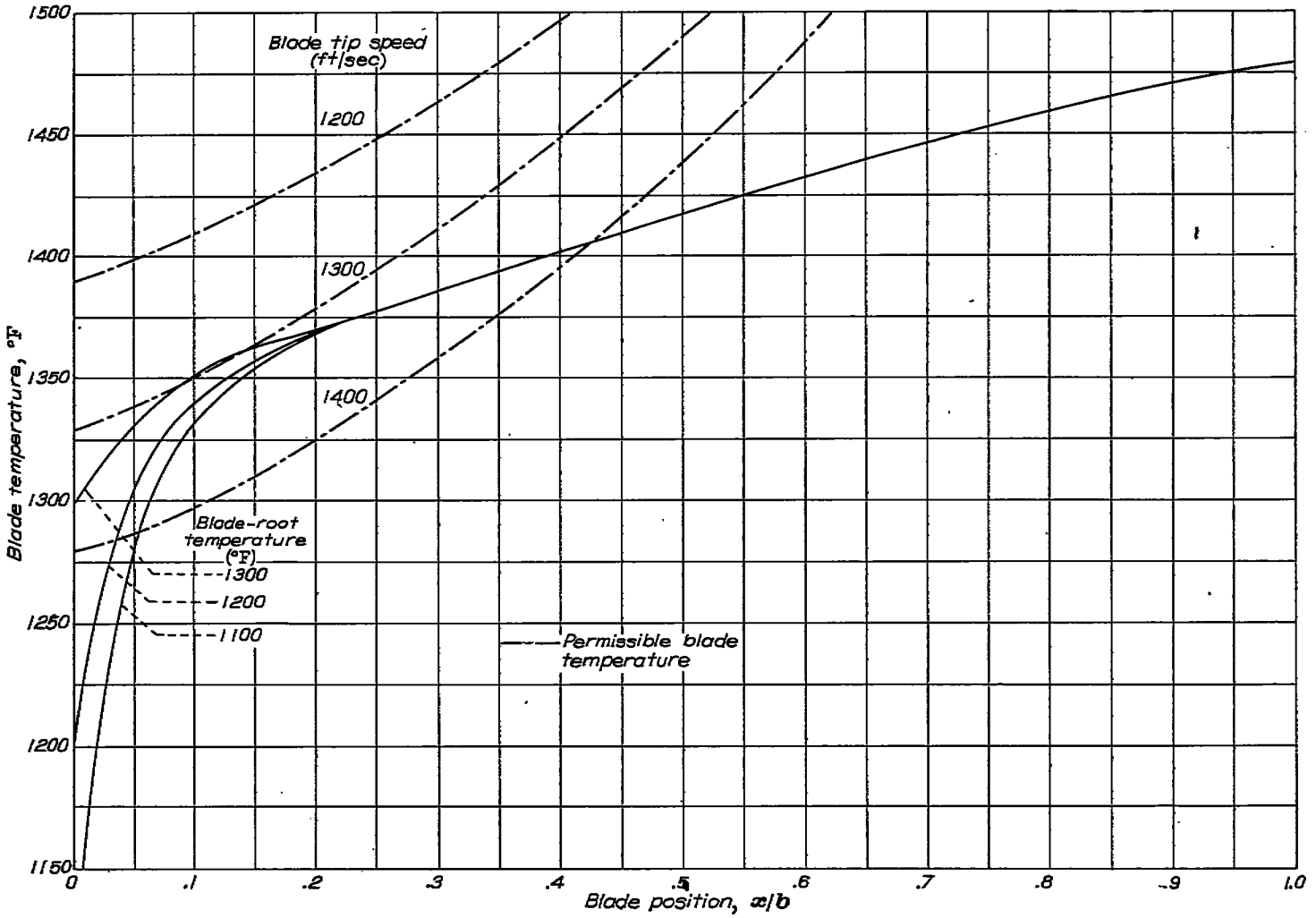

FIGURE 8.—Effect on temperature distribution of change in blade-root temperature for insert blade. Effective gas temperature, 1900° F; blade-root cooling-air temperature, 400° F: average insert temperature, 700° F; coolant-flow ratio, 0.03.

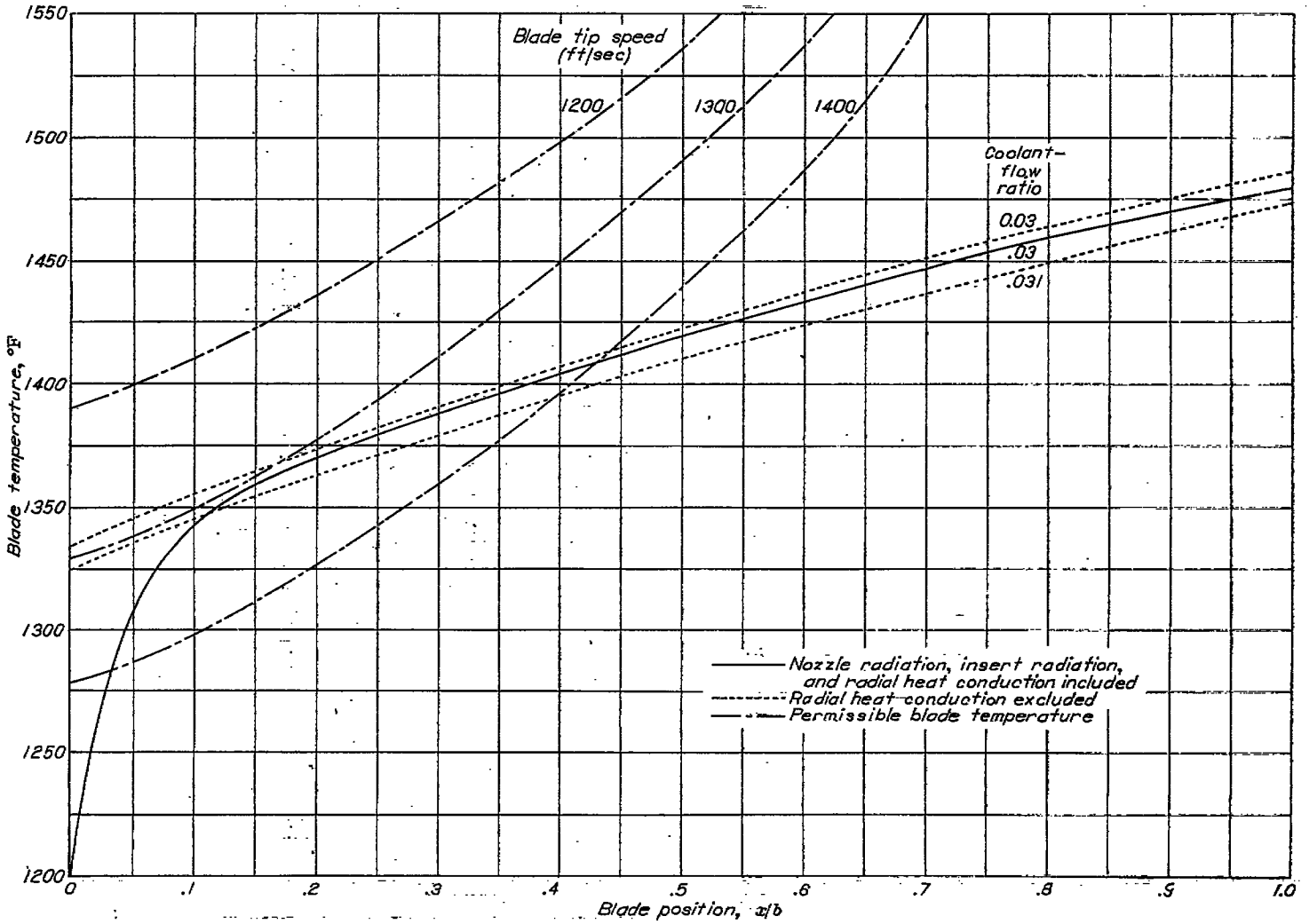

FIGURE 9.—Effect on temperature distribution and coolant-flow ratio of neglecting radial heat conduction in insert blade. Effective gas temperature, 1900° F; blade-root cooling-air temperature, 400° F; average insert temperature, 700° F.

RESULTS OF SOLUTION OF CASE II

The results of an investigation for case II, which includes cooling-air-temperature change due to heat transfer and rotation and radiation but which neglects radial conduction, is now given for the insert blade. For this investigation, equation (11), which is a first-order linear differential equation that replaces the third-order equation (4) when conduction is neglected, was applied. In figure 9, the temperature distribution obtained when radial conduction is neglected is compared with that when conduction is included. The result of neglecting radial conduction is to overestimate the blade temperature; hence, a slight increase in required coolant-flow ratio results. In addition, when radial conduction is neglected, the critical blade point is nearer the blade root.

Because the result of neglecting radial conduction resulted in an overestimation of the blade temperature and because it was believed that the result of neglecting radiation would be to underestimate the blade temperature, an example is presented to show the result of neglecting both conduction and radiation. The results are shown in figure 10. Although the combined effects of neglecting both radiation and radial heat conduction result in a slight underestimation of the blade temperature, it was decided to use the simpler temperature-distribution equation (equation (18)) in further investigations. It was this decision that led to the construction of the nondimensional charts shown in figures 4 and 5.

SOLUTION OF CASE III BY USE OF CHARTS

In order to illustrate the use of the nondimensional charts, which were constructed so as to yield the same temperature distribution as would be obtained by use of equation (18), a 25-fin air-cooled blade is considered. The numerical values used in the calculations are given in the section entitled "Illustrative Examples;" an effective gas temperature of 1900° F, a blade-root cooling-air temperature of 400° F, and a coolant-flow ratio of 0.03 are assumed. The inside heat-transfer coefficient h_i, involving the total internal surface area (fins and blade-wall areas), is determined in the usual manner from the following equation:

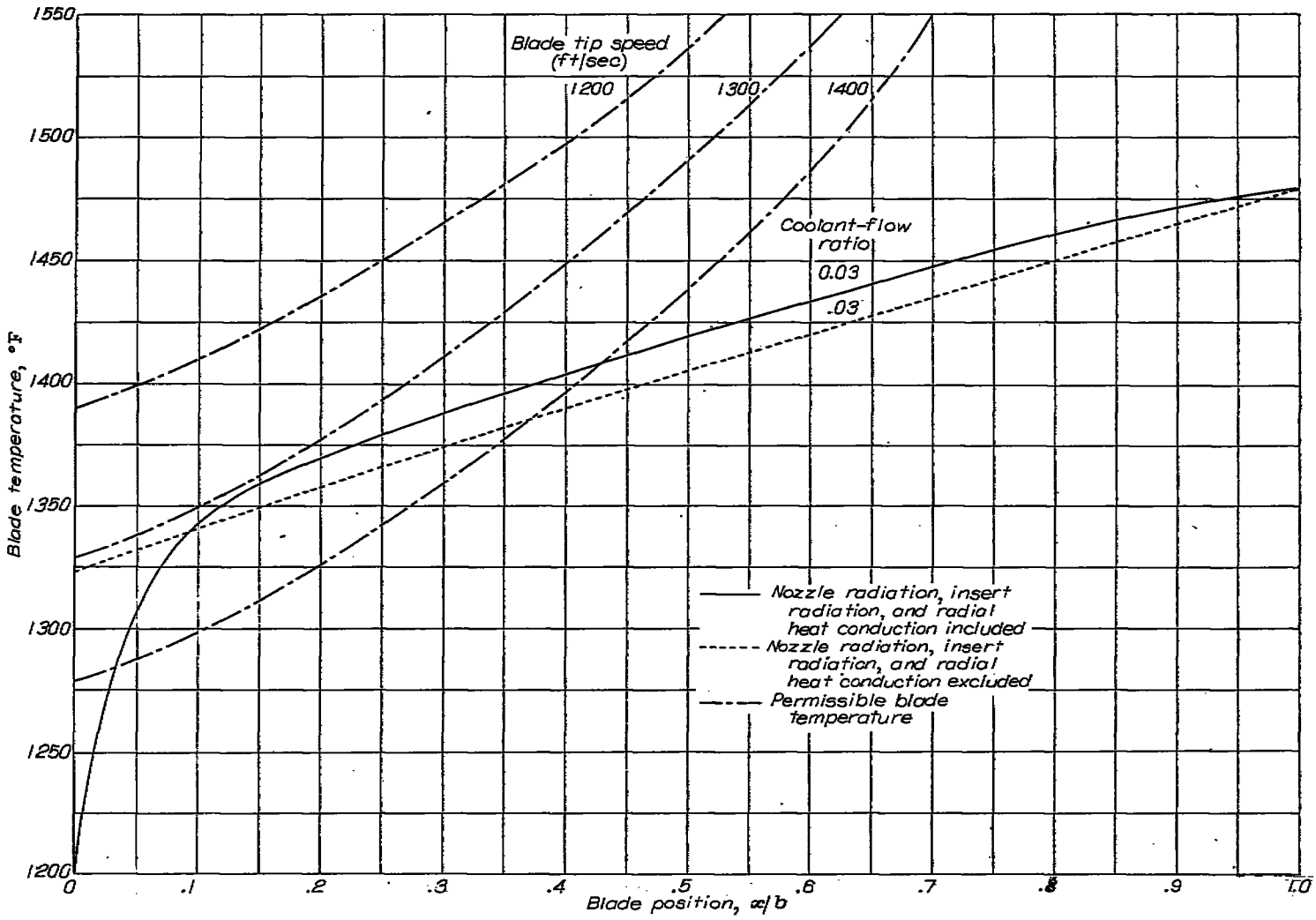

FIGURE 10.—Effect on temperature distribution and coolant-flow ratio of neglecting radiation from stator blades to turbine-blade wall, radiation from inner blade wall to insert, and radial heat conduction in insert blade. Effective gas temperature, 1900° F; blade-root cooling-air temperature, 400° F; average insert temperature, 700° F.

$$h_i=\frac{0.00288}{A_c}(l_c)^{0.2}(w_a)^{0.8}$$

$$=0.00288\left(\frac{1.07}{0.00147}\right)^{0.2}\left(\frac{158}{0.00147}\right)^{0.8}$$

$$=(0.00288)(728)^{0.2}(107{,}300)^{0.8}$$

$$=(0.00288)(3.74)(10{,}600)$$

$$=114\text{ Btu/(hr)(°F)(sq ft)}$$

$$=114/3600\text{ Btu/(sec)(°F)(sq ft)}$$

The over-all inside heat-transfer coefficient, based only on the inner blade surface area, is now calculated. The value of

$$\phi_f=\sqrt{\frac{2h_i}{k_B\tau_f}}$$

is found to be

$$\phi_f=\sqrt{\frac{2(114)(3600)}{12(0.0017)(3600)}}=\sqrt{11{,}200}=106\,(\text{ft})^{-1}$$

and the over-all coefficient h_f is

$$h_f=\frac{h_i}{m+\tau_f}\left(\frac{2\tanh\phi_f L_f}{\phi_f}+m\right)$$

$$=\frac{114}{(0.0035+0.0017)}\left[\frac{2\tanh(106)(0.009)}{106}+0.0035\right]$$

$$=\frac{114}{0.0052}\left[\frac{2(0.740)}{106}+0.0035\right]$$

$$=\frac{114}{0.0052}(0.0140+0.0035)$$

$$=\frac{114}{0.0052}0.0175$$

$$=383\text{ Btu/(hr)(°F)(sq ft)}$$

$$=383/3600\text{ Btu/(sec)(°F)(sq ft)}$$

The parameters necessary for application of the nondimensional chart are:

$$\lambda=\frac{h_o l_o}{h_f l_t}=\frac{(198)(0.385)(3600)}{(383)(0.314)(3600)}=0.634$$

(In the definition of λ here, h_f replaces h_t.)

$$\frac{1}{1+\lambda}=\frac{1}{1.634}=0.612$$

$$\frac{h_o l_o b}{c_p w_a}=\frac{(198)(0.385)(0.333)(3600)}{(0.241)(158)(3600)}=0.667$$

$$\frac{1}{1+\lambda}\frac{h_o l_o b}{c_p w_a}=(0.612)(0.667)=0.409$$

$$\frac{\omega^2 w_a}{gJh_o l_o(T_{g,e}-T_{a,e,r})}=\frac{(1200)^2(158)(3600)}{(32.2)(778)(198)(0.385)(1500)(3600)}=0.0794\ (\text{ft})^{-1}$$

$$\left[\frac{c_p w_a(1+\lambda)}{h_o l_o}-r_r\right]=\frac{(0.241)(158)(1.634)}{(198)(0.385)}=0.75$$
$$=0.815-0.750=0.065\ (\text{ft})$$

The spanwise temperature distribution through the 25-fin blade is determined as follows: The value 0.667 is located as the abscissa in quadrant I of figure 4(a); a vertical line is constructed through this point intersecting the family of lines representing x/b. From each of these intersections, horizontal lines are drawn to intersect the quadrant II line representing $1/(1+\lambda)=0.612$. A sample path is shown in figure 4(a). These intersections are then connected by vertical lines to quadrant III to the curve that gives the value of the exponential function as the ordinate. Horizontal lines from these exponential values to the line representing $1/(1+\lambda)=0.612$ in quadrant IV yield the desired first term of equation (18) $\frac{1}{1+\lambda}e^{-\left(\frac{1}{1+\lambda}\frac{h_o l_o b}{c_p w_a}\frac{x}{b}\right)}$, on the horizontal axis at the bottom quadrant IV. For the 25-fin blade, this first term representing the heat transferred by the blade was found to be

	for $\frac{x}{b}$
0.612	0
.560	.2
.515	.4
.475	.6
.440	.8
.405	1.0

The third term in equation (18)

$$\left[1-e^{-\left(\frac{1}{1+\lambda}\frac{h_o l_o b}{c_p w_a}\frac{x}{b}\right)}\right]\left[\frac{\omega^2 w_a}{gJh_o l_o(T_{g,e}-T_{a,e,r})}\right]\left[\frac{c_p w_a(1+\lambda)}{h_o l_o}-r_r\right]$$

can now be determined from figure 4(b). The values of the abscissas in quadrant I are determined by subtracting from 1 the ordinate in quadrant III of figure 4(a) for the respective values of x/b. (This ordinate has just been determined.) The parameter

$$\frac{\omega^2 w_a}{gJh_o l_o(T_{g,e}-T_{a,e,r})}$$

for this case is 0.0794 and intersections with this line by vertical lines through the previously determined abscissas locate the desired points in quadrant I. These points are joined by horizontal lines to the line in quadrant II representing the parameter

$$\frac{c_p w_a(1+\lambda)}{h_o l_o}-r_r=0.065$$

A sample path is shown on figure 4(b). The corresponding abscissas are the desired values, that is, the values of the third term in equation (18). In this particular case, these values are all less than 0.0018.

The second term in equation (18) represents the effect of the centrifugal compression of the air and is obtained by multiplication of the parameter in quadrant I of figure 4(b) by the appropriate value of x. For the problem under consideration, the values of x are 0.333 times the value of x/b considered. For the example being considered, these values are less than 0.027. Insertion of the values just found into equation (18) results in

$\frac{x}{b}$	$\frac{1900-T_B}{1900-400}$	T_B (°F)
0	0.612	977
.2	.560−0.0053+0.0004	1007
.4	.515− .0106+ .0008	1144
.6	.475− .0158+ .0011	1210
.8	.440− .0211+ .0014	1270
1.0	.405− .0265+ .0018	1328

This temperature distribution is shown as the lower curve of figure 11.

A similar calculation was made for the insert blade, under the same hypotheses as those used for the finned blade. The inside heat-transfer coefficient for the insert blade was already found to be $\frac{151}{3600}$ Btu/(sec) (°F) (sq ft). The values of the parameters $\frac{h_o l_o b}{c_p w_a}$ and $\frac{\omega^2 w_a b}{gJh_o l_o(T_{g,e}-T_{a,e,r})}$ are unchanged, but because of the change in the value of h_t, a new value of λ ($\lambda=1.607$) results. Therefore,

$$\frac{1}{1+\lambda}=0.384$$

$$\frac{1}{1+\lambda}\frac{h_c l_c b}{c_p w_a}=(0.384)\ (0.667)=0.256$$

$$\frac{c_p w_a(1+\lambda)}{h_c l_c}-r_r=\frac{(0.241)\ (158)\ (2.607)\ (3600)}{(3600)\ (198)\ (0.385)}-0.75$$

$$=1.302-0.75$$

$$=0.552\ \text{(ft)}$$

The use of figure 4 and the accompanying necessary simple calculation gave the following results for the insert blade:

$\frac{x}{b}$	$\frac{1900-T_B}{1900-400}$	T_B (°F)
0	0.384	1324
.2	.365−0.005+0.002	1358
.4	.347− .011+ .004	1390
.6	.330− .016+ .006	1420
.8	.313− .021+ .003	1450
1.0	.297− .027+ .010	1480

This temperature distribution is shown as the upper curve on figure 11; it is about 350° F higher at the blade root and 150° F higher at the blade tip than the curve for the 25-fin blade.

A comparison of these results with those for the finned blade shows that by decreasing the inside heat-transfer coefficient, an increase in blade temperature results; that is, the contribution from figure 4(a) decreases whereas that from figure 4(b) increases, but because the contribution of figure 4(a) is predominating, increased temperatures result.

DISCUSSION

An equation is derived for calculating the spanwise blade-temperature distribution for an air-cooled hollow blade with an insert when the heat transfer by convection, conduction, and radiation, and the heat of compression are considered. Modifications in this equation necessary for its application to hollow air-cooled blades and internally finned air-cooled blades are noted. Simplified equations are also obtained by neglecting, in turn, conduction; conduction and radiation; and conduction, radiation, and the heat of compression. Finally, a simplified equation giving an average metal temperature corresponding to an average air temperature is obtained.

A comparison of temperature distributions, obtained for the most general case (case I), reveals that for the insert blade considered the required coolant-flow ratio was only about one-fourth that required for the hollow blade. By use of the nondimensional charts for a simplified temperature equation for a fixed set of conditions, the temperatures in a

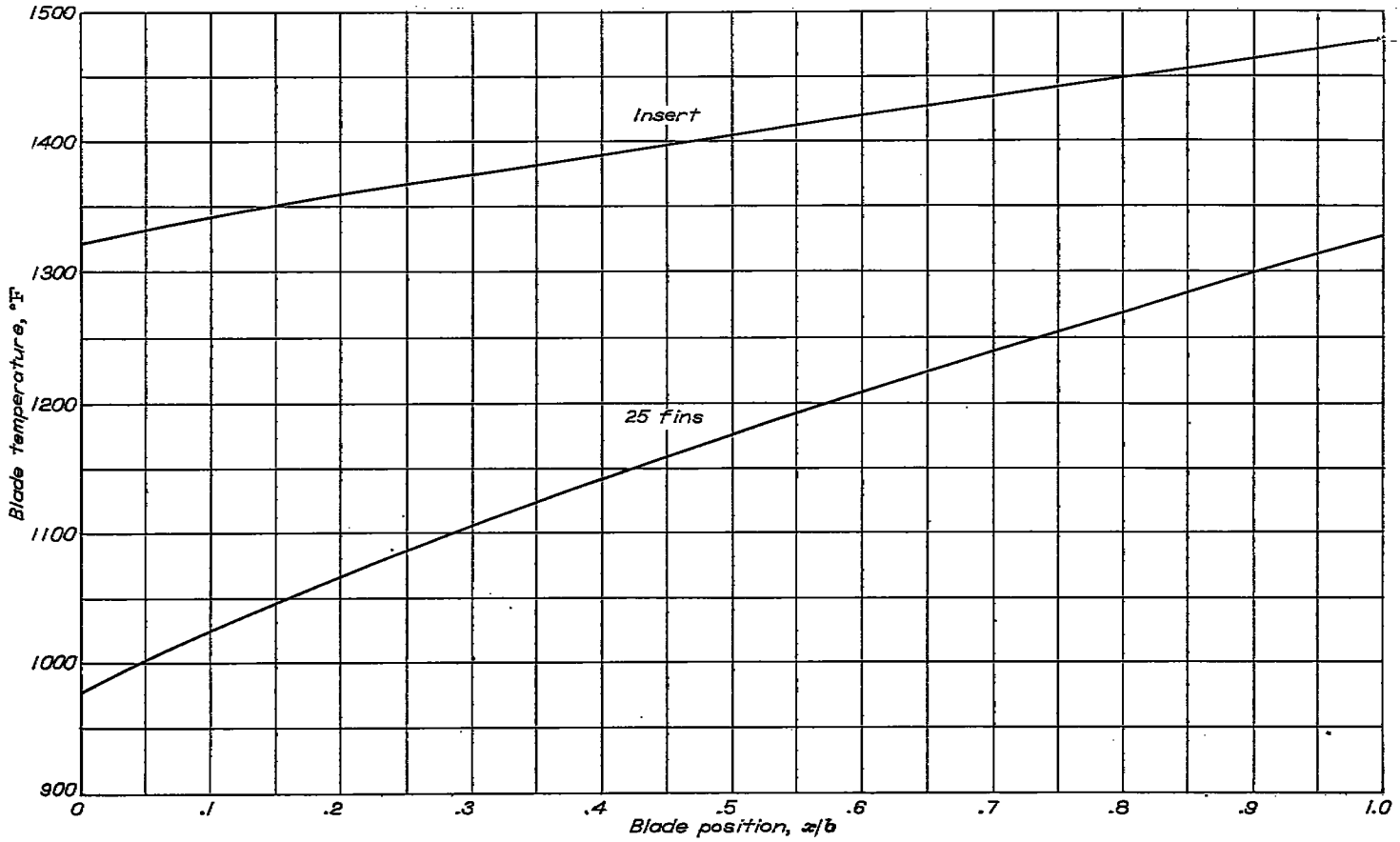

FIGURE 11.—Temperature distribution through insert and 25-fin air-cooled turbine blades, including only cooling-air-temperature change due to heat transfer and rotation. Effective gas temperature, 1900° F; blade-root cooling-air temperature, 400° F; coolant-flow ratio, 0.03.

25-fin blade are also shown to be less than those in a blade with an insert by about 350° F at the blade root and about 150° F at the blade tip.

The result of an investigation of the effect of neglecting radial conduction (which results in reducing the order of the differential equation from three to one and hence in simplifying the solution) on the temperature distribution through the insert blade shows that when conduction is neglected a slight overestimation of the blade temperature is obtained. By neglecting both radial conduction and radiation, however, a slight underestimation of the blade temperature results because of the counteracting influences of conduction and radiation on the temperature distributions. Because this result was found to be true for the large number of passages studied, it was determined that representative results could be obtained by use of the nondimensional charts.

Temperature distributions through the insert blade and the 25-fin blade are determined by use of these charts. These distributions reveal that the term representing the heat transferred by the blade predominates. For the examples considered, this term is more than 10 times as large as the term representing the effect of centrifugal compression of the air.

These results, although limited to a small range of shapes and temperatures, indicate that, at least for certain conditions, spanwise blade-temperature distributions may be very easily obtained by use of the greatly simplified equations or nondimensional charts.

CONCLUDING REMARKS

Spanwise temperature-distribution equations are derived for air-cooled hollow blades, air-cooled hollow blades with inserts, and internally finned air-cooled blades. The cooling-air-temperature changes due to heat transfer and rotation, radiation, and radial conduction are initially considered, and are then omitted in turn. Simplified equations result from these omissions. One method is presented for obtaining an approximate stress-limited allowable blade-temperature distribution and the cooling-air requirements.

Results of several numerical examples that are included indicate that the simplified equations give sufficiently accurate results for a wide range of configurations. In order to facilitate the obtaining of solutions for these simplified cases, nondimensional charts are developed. By use of these charts, simplified solutions can be obtained with a minimum of calculation. Two numerical illustrations demonstrating the use of the nondimensional charts are presented.

LEWIS FLIGHT PROPULSION LABORATORY,

NATIONAL ADVISORY COMMITTEE FOR AERONAUTICS,

CLEVELAND, OHIO, *March 1, 1950.*

APPENDIX A

SYMBOLS

The following symbols are used in the calculations and the figures:

A	cross-sectional area, sq ft
b	blade height or span, ft
$C_1, \ldots C_5$	integration constants
c_p	specific heat at constant pressure, Btu/(lb) (°F)
D	operator denoting differentiation
D_h	hydraulic diameter, ft
F	number of fins
G	mass velocity, lb/(sec) (sq ft)
G_1	$\frac{h_s l_t}{k_B l_{B,av} \tau_{B,w}}$, $(\text{ft})^{-2}$
G_2	$\frac{h_i l_i}{k_B l_{B,av} \tau_{B,w}}$, $(\text{ft})^{-2}$
G_2'	$\frac{h_f l_i}{k_B (l_{B,av} \tau_{B,w} + 2 L_f \tau_f F)}$, $(\text{ft})^{-2}$
G_3	$\frac{h_N L_e + h_o l_o}{k_B l_{B,av} \tau_{B,w}}$, $(\text{ft})^{-2}$
G_3'	$\frac{h_N L_e + h_o l_o}{k_B (l_{B,av} \tau_{B,w} + 2 L_f \tau_f F)}$, $(\text{ft})^{-2}$
g	acceleration due to gravity, ft/sec ^{2}
h	heat-transfer coefficient, Btu/(sec) (°F) (sq ft)
J	mechanical equivalent of heat, 778 ft-lb/Btu
k	thermal conductivity, Btu/(sec) (°F) (ft)
L_e	effective blade width, ft
L_f	effective fin width, ft
l	perimeter, ft
m	average distance between fins, ft
Q	heat-flow rate, Btu/sec
Q_1	heat entering by conduction, Btu/sec
Q_2	heat leaving by conduction, Btu/sec
Q_3	heat entering by radiation from nozzles and by convection, Btu/sec
Q_4	heat leaving by radiation to insert and by convection, Btu/sec
r	radius, ft
T	static temperature, °F
T''	total temperature, °F
u	tip speed, ft/sec
W	velocity of cooling air relative to blades, ft/sec
w	weight-flow rate, lb/sec
x	distance from blade root to blade element, ft
Y_1	$\frac{h_i(l_i + l_s)}{c_p w_a}$, $(\text{ft})^{-1}$
Y_2	$\frac{h_i l_i}{h_N L_e + h_o l_o + h_i l_i + h_s l_i}$
Y_2'	$\frac{h_i l_i}{h_N L_e + h_o l_o + h_i l_i}$
Y_2''	$\frac{h_f l_i}{h_N L_e + h_o l_o + h_f l_i}$
ζ	$(r - r_r)\sqrt{\frac{h_o l_o + h_i l_i}{k_B A_{B,w}}}$
λ	$\frac{h_o l_o}{h_i l_i}$
μ	viscosity, lb/(sec) (ft)
τ	thickness, ft
ϕ_f	$\sqrt{\frac{2h_i}{k_B \tau_f}}$, $(\text{ft})^{-1}$
ω	angular velocity, radians/sec

Subscripts:

a	air
av	average
B	blade
c	coolant passage
e	effective
f	fin
g	gas
i	inside
max	maximum
N	nozzle
o	outside
r	blade root
s	insert
T	blade tip
w	wall

APPENDIX B

ONE-DIMENSIONAL SPANWISE TEMPERATURE DISTRIBUTION FOR AIR-COOLED HOLLOW TURBINE BLADE WITH INSERT

A heat balance for a small section of the blade height dx follows (fig. 2):

$$Q_1 = k_B l_{B,av} \tau_{B,w} \frac{d}{dx}\left(T_B + \frac{dT_B}{dx} dx\right)$$

$$Q_2 = k_B l_{B,av} \tau_{B,w} \frac{dT_B}{dx}$$

$$Q_3 = (h_N L_e + h_o l_o)(T_{g,e} - T_B) dx$$

(See reference 3.)

$$Q_4 = h_i l_i (T_B - T_{a,e}) dx + h_s l_i (T_B - T_s) dx$$

where

Q_1 heat entering by conduction
Q_2 heat leaving by conduction
Q_3 heat entering by radiation from nozzles and by convection
Q_4 heat leaving by radiation to insert and by convection

and where $T_{a,e}$ is the adiabatic temperature of the inner blade wall.

The heat balance requires

$$Q_1-Q_2+Q_3-Q_4=0$$

which reduces to

$$k_B l_{B,av} \tau_{B,av} \frac{d^2T_B}{dx^2}+(h_N L_e+h_o l_o)(T_{g,e}-T_B)=$$

$$h_i l_i (T_B-T_{a,e})+h_s l_i (T_B-T_s) \quad (1)$$

or

$$\frac{d^2T_B}{dx^2}-(G_1+G_2+G_3)T_B+G_2T_{a,e}+G_1T_s+G_3T_{g,e}=0 \quad (B1)$$

where

$$G_1=\frac{h_s l_i}{k_B l_{B,av} \tau_{B,w}}$$

$$G_2=\frac{h_i l_i}{k_B l_{B,av} \tau_{B,w}}$$

$$G_3=\frac{h_N L_e+h_o l_o}{k_B l_{B,av} \tau_{B,w}}$$

The next step in the derivation of the desired temperature-distribution equation is the elimination of the quantity $T_{a,e}$, which can be accomplished by solving equation (B1) for $T_{a,e}$, differentiating the resulting equation, and equating this derivative to the total rise in cooling-air temperature due to heat transferred by the blades and to the compression of the air in the blades by centrifugal force. The two expressions for $dT_{a,e}/dx$ are as follows: In the expression for $dT_{a,e}/dx$, it is necessary also to remove $T_{a,e}$ by substituting its value obtained from equation (B1).

From equation (B1),

$$T_{a,e}=-\frac{1}{G_2}\frac{d^2T_B}{dx^2}+\frac{1}{G_2}(G_1+G_2+G_3)T_B-\frac{G_1}{G_2}T_s-\frac{G_3}{G_2}T_{g,e} \quad (B2)$$

Differentiation of equation (B2) gives

$$\frac{dT_{a,e}}{dx}=-\frac{1}{G_2}\frac{d^3T_B}{dx^3}+\frac{1}{G_2}(G_1+G_2+G_3)\frac{dT_B}{dx} \quad (2)$$

The total rise in cooling-air temperature relative to the blades is due to the heat transferred by the blades and to the compression of the air in the blades by centrifugal force. The temperature rise due to the heat transferred by the blades is

$$c_p w_a dT_{a,e}=h_i l_i (T_B-T_{a,e})dx+h_i l_s (T_s-T_{a,e})dx$$

or

$$\frac{dT_{a,e}}{dx}=\frac{h_i l_i}{c_p w_a}T_B-\frac{h_i(l_i+l_s)}{c_p w_a}T_{a,e}+\frac{h_i l_s}{c_p w_a}T_s \quad (B3)$$

The temperature rise due to compression in the blade is obtained by assuming the small increment in effective temperature $dT_{a,e}$ equal to the small increment in cooling-air total temperature dT''_a. Because the cooling-air total temperature is defined by

$$T''_a=T_a+\frac{W^2}{2gJc_p}$$

where W is the velocity of cooling air relative to the blade coolant passage, the temperature rise due to compression in the blade is

$$dT_{a,e}=\frac{\omega^2 r\,dr}{gJc_p}$$

or

$$\frac{dT_{a,e}}{dx}=\frac{\omega^2(r_r+x)}{gJc_p} \quad (B4)$$

where x is defined by the relation

$$r=r_r+x$$

Thus, the total rise in cooling-air temperature is the sum of equations (B3) and (B4); that is,

$$\frac{dT_{a,e}}{dx}=\frac{h_i l_i}{c_p w_a}T_B-\frac{h_i(l_i+l_s)}{c_p w_a}T_{a,e}+\frac{h_i l_s}{c_p w_a}T_s+\frac{\omega^2(r_r+x)}{gJc_p} \quad (3)$$

Equating equations (2) and (3), substituting equation (B2) in equation (3), and simplifying lead to the desired equation

$$\frac{d^3T_B}{dx^3}+Y_1\frac{d^2T_B}{dx^2}-(G_1+G_2+G_3)\frac{dT_B}{dx}+\left[\frac{h_i l_i}{c_p w_a}G_2-Y_1(G_1+G_2+G_3)\right]T_B=-\frac{\omega^2 G_2}{gJc_p}x-\left[\frac{\omega^2 G_2}{gJc_p}r_r+\left(\frac{h_i l_s}{c_p w_a}G_2+Y_1G_1\right)T_s+Y_1G_3T_{g,e}\right] \quad (4)$$

where

$$Y_1=\frac{h_i(l_i+l_s)}{c_p w_a}$$

REFERENCES

1. McAdams, William H.: Heat Transmission. McGraw-Hill Book Co., Inc., 2d ed., 1942, pp. 170, 232.
2. Kells, Lyman M.: Elementary Differential Equations. McGraw-Hill Book Co., Inc., 2d ed., 1935.
3. Harper, D. R., 3d, and Brown, W. B.: Mathematical Equations for Heat Conduction in the Fins of Air-Cooled Engines. NACA Rep. 158, 1922.
4. Brown, W. Byron, and Livingood, John N. B.: Cooling of Gas Turbines. III—Analysis of Rotor and Blade Temperatures in Liquid-Cooled Gas Turbines. NACA RM E7B11c, 1947.
5. Wolfenstein, Lincoln, Maxwell, Robert L., and McCarthy, John S.: Cooling of Gas Turbines. V—Effectiveness of Air Cooling of Hollow Blades. NACA RM E7B11e, 1947.
6. Lowdermilk, Warren G., and Grele, Milton D.: Heat Transfer from High-Temperature Surfaces to Fluids. II—Correlation of Heat-Transfer and Friction Data for Air Flowing in Inconel Tube with Rounded Entrance. NACA RM E8L03, 1949.